Stereochemistry and Near-Infrared Circular Dichroism of a Chiral Yb Complex

Lorenzo Di Bari,[†] Guido Pintacuda,[†,‡] and Piero Salvadori*[,†]

Contribution from the Dipartimento di Chimica e Chimica Industriale, Centro di Studio del CNR per le Macromolecole Stereoordinate ed Otticamente Attive, Via Risorgimento 35, I-56126 Pisa, Italy, and Scuola Normale Superiore, Piazza dei Cavalieri 7, I-56126 Pisa, Italy

Received December 7, 1999. Revised Manuscript Received March 28, 2000

Abstract: The near-infrared CD spectrum of ytterbium complexed by DOTMA, [DOTMA = (1*R*,4*R*,7*R*,10*R*)-α,α′,α″,α‴-tetramethyl-1,4,7,10-tetraazacyclododecane-1,4,7,10-tetraacetic acid)] is presented. This is the first report of a near-infrared CD spectrum in solution of the f−f transitions of ytterbium in a complex whose solution structure and dynamics are completely defined. The spectrum shows several well-resolved transitions around 980 nm with very high dissymmetry factors. In water and in methanol, there are two diastereomeric conformations of YbDOTMA in equilibrium, Λ(*δδδδ*) or *n* and Λ(*λλλλ*) or *p*, being the latter always in a large excess. The relative proportion depends on temperature and solvent composition, but the CD spectrum is rather insensitive to these parameters, which demonstrates that neglecting the minor form contribution is an acceptable approximation. On lowering the temperature, the presence of *hot bands* is highlighted, which leads to a tentative assignment of the transitions. The absorption counterpart compares very well with that of YbDOTA, an achiral analogue, largely studied and well understood.

Introduction

Structural and dynamic studies on lanthanide ion complexes are nowadays growing quickly, largely because of the new and broad applications these systems find both in chemistry and in biomedical sciences.[1,2] Indeed, these metals provide excellent catalysts for several reactions and there are reports of promising stereoselective reactions promoted by chiral nonracemic lanthanide complexes.[3] Furthermore, when coordinated with ligands based on N-alkylated polyamine, Ln(III) ions (particularly Gd^{3+}) find widespread applications in diagnostics and therapy, e.g. as powerful contrast agents in MRI.[2] One of the big challenges in this field is the design of tissue-selective agents, which are recognized by specific receptors, enhancing the contrast with nearby areas.

In the case of enantioselective auxiliaries in chemistry as well as following interaction between an achiral contrast agent and a receptor,[4] the lanthanide ion experiences a dissymmetrical environment, which leads one to the obvious attempt to use circular dichroism and circularly polarized luminescence spectroscopy to characterize the absolute stereochemistry.

Lanthanides offer very peculiar spectroscopic properties, due to the partial population of the f-orbitals, and lend themselves to versatile and sensitive investigation methods. The f−f transitions very often occur in rather unusual regions of the spectrum, where there are very few and often negligible contributions from other chromophores. Strictly speaking, they are electrically forbidden, and often magnetically allowed, which ensures small extinction coefficients, making the detection of the CD spectrum easy. An enormous amount of work has been devoted to the measurement and analyses of the $4f^N$ electronic state structures of trivalent lanthanide ions in crystals, with the leading contribution of Richardson and co-workers.[5−8] Solution data on the optical properties of coordination compounds of lanthanides would lend themselves to several uses in different areas of modern chemistry.[9−12] Unfortunately, results in solution are much less abundant and rationalized. Owing to the small crystal fields of the ligands, electronic lines are superimposed in solution and a large amount of potentially useful information is lost. Among other problems, there is the need of a precise knowledge of the structure and possibly of the dynamic processes in solution. From this point of view, one of the best suited lanthanide systems is undoubtedy ytterbium(III), since its properties in nuclear magnetic resonance[13] enable a clear description of the molecular geometry surrounding the ion.

The electronic spectrum of ytterbium is characterized by one intraconfigurational manifold ($^2F_{7/2} \rightarrow {}^2F_{5/2}$) in the near-infrared (NIR) around 980 nm. This transition is magnetically allowed ($|\Delta J| = 1$), which implies that it is particularly suited for CD

[†] Centro di Studio del CNR per le Macromolecole Stereoordinate ed Otticamente Attive.

[‡] Scuola Normale Superiore.

(1) Evans, C. H. *Biochemistry of the Lanthanides*; Plenum Press: New York, 1990.

(2) Aime, S.; Botta, M.; Fasano, M.; Terreno, E. *Chem. Soc. Rev.* **1998**, *27*, 19−29.

(3) Kobayashy, S., Ed. *Lanthanides: Chemistry and Use in Organic Synthesis*; Springer-Verlag: Berlin, 1999; and references therein.

(4) Actually, many contrast agents currently used in MRI proctice *are* chiral and very often racemic. This is indeed surprising given the stress that chiral discriminations should have in medicinal chemistry.

(5) Reid, M. F.; Richardson, F. S. *J. Phys. Chem.* **1984**, *88*, 3579−3586.

(6) Richardson, F. S.; Berry, M. T.; Reid, M. F. *Mol. Phys.* **1986**, *58*, 929−945.

(7) Berry, M. T.; Schwieters, C.; Richardson, F. S. *Chem. Phys.* **1988**, *122*, 125−139.

(8) Moran, D. M.; Richardson, F. S. *Inorg. Chem.* **1992**, *31*, 813−818.

(9) Brittain, H. G. *Coord. Chem. Rev.* **1983**, *48*, 243−276.

(10) Parker, D.; Gareth Williams, J. A. G. *J. Chem. Soc., Dalton Trans.* **1996**, 3613−3629.

(11) Dillon, J.; Nakanishi, K. *J. Am. Chem. Soc.* **1975**, *97*, 5409−5423.

(12) Tsukube, H.; Hosokubo, M.; Wada, M.; Shinoda, S.; Tamiaki, H. *J. Chem. Soc., Dalton Trans.* **1999**, 11−12.

(13) Bertini, I.; Luchinat, C. *Coord. Chem. Rev.* **1996**, *150*, 1−296.

10.1021/ja994290z CCC: $19.00 © 2000 American Chemical Society
Published on Web 05/27/2000

Scheme 1

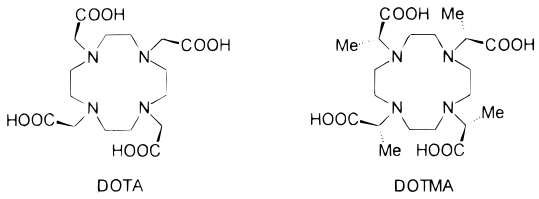

spectroscopy.[14] Nowadays, commercial dichrographs extending the wavelength range to 1100 nm are available, which opens the field of chiroptical spectroscopy of ytterbium. There are very few reports of CD and CPL of ytterbium in the literature[15−18] and no interpretation of the spectra was attempted, because no accurate information on the stereochemistry *in solution* was available. The present study takes as its objective a molecule that is very well structurally characterized, Yb DOTMA,[19] a chiral analogue of one of the most successful contrast agents for MRI, Gd DOTA.[19] The presence of four homochiral methyl acetate branches dictates the absolute stereochemistry of the coordination polyhedron, which is reflected in the signs and amplitudes of the dichroic bands, allowing for a clear relationship between observed CD and structure in solution.

An investigation of the electronic properties of lanthanide complexes of such a molecule was reported,[20] but interest was centered almost exclusively on the Eu(III) and Tb(III) complexes and a correlation of the observed spectra with plausible structures was impossible because of the complex nature of the electronic levels of such ions and the lacking characterization of the solution dynamics of the species.

To approach a rationalization of the electronic spectrum, a detailed knowledge of the solution structure and equilibria is a prerequisite. On the grounds of the preliminary report of Brittain and Desreux,[20] we recently published[21] such a study and in the following we briefly summarize the results that can be useful for the interpretation of the CD spectrum of Yb DOTMA.

Solution Structure and Equilibria of Yb DOTMA. As for several complexes based on N-alkylated cyclen ligands, the proton NMR spectrum reveals that in acqueous solution Yb DOTMA is subject to a slow (on the NMR time scale) equilibrium between two forms, which are in a ratio of about 10:1.[20,21]

The structures of the two interconverting complexes feature C_4 symmetry and differ for the layout of the macrocycle, which can be ($\lambda\lambda\lambda\lambda$) or ($\delta\delta\delta\delta$). No rotation of the methyl acetate arm can be observed, instead, and the helicity of the coordination polyhedron is Λ in both species. The inversion of the cyclen ring swaps protons between equivalent positions, which implies that the two sets of geometrical factors are practically equal and that the assignment of the major/minor component on the basis of pseudocontact shifts only is particularly unsafe. Moreover, it has been demonstrated that minor geometrical adjustments can account for residual deviations between calculated (e.g. on the basis of crystal structure) and observed pseudocontact shifts.[22]

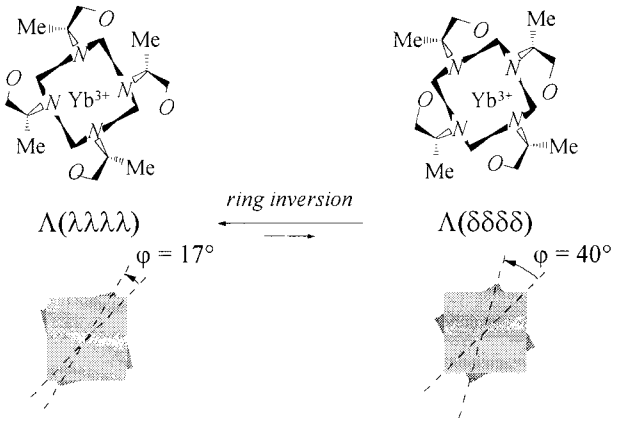

Figure 1. Solution equilibrium in YbDOTMA. Bottom: Schematic representation of the coordination polyhedron: at the corners of the light gray squares are the oxygens and at the corners of the dark ones the nitrogen atoms; the tilt angle φ between the two squares is also indicated. The water molecule axially coordinated in the minor form is not depicted.

Independent information comes from NOE measurements. In such a way, internuclear distances between protons in the major form can be estimated and one can assign it to the $\Lambda(\lambda\lambda\lambda\lambda)$ or *p*-form.[23] This is just opposite to what is found for YbDOTA,[22,24] where the *n*-form is the most abundant one. The situation can be depicted as in Figure 1.

The thermodynamic parameters for the equilibrium in methanol are

$$\Delta H^\circ = -4 \text{ kJ mol}^{-1}$$

$$\Delta S^\circ = -35 \text{ J K}^{-1} \text{ mol}^{-1}$$

The *negative* entropy on going from the major to minor form is very similar to what is found for the reverse process in Yb DOTA.[25] It can be interpreted with the uptake of a water molecule, which should be axially coordinated to the *p* isomer.

The two species in equilibrium do not differ only in conformation, but even in the structure of the coordination polyhedron, which consists of a distorted square antiprism, monocapped for the *p*-form. Furthermore, the degree of distortion is largely different: the squares of the oxygens and of the nitrogens are skewed by 40° in the *p*-form and 17° in the *n*-form, as shown in Figure 1. This has very important consequences on the electronic spectrum, which will be discussed below.

Finally, it can be observed that the two sets of ^{1}H NMR signals for the two forms are characterized by largely different anisotropy factors, D:

$$D_p = 3200 \pm 90$$

$$D_n = 5300 \pm 100$$

According to Bleaney's theory,[26,27] this should imply an analogous difference in the cristal-field parameter B_0^2, which

(14) Richardson, F. S. *Inorg. Chem.* **1980**, *19*, 2806−2812.
(15) Salvadori, P.; Rosini, C.; Bertucci, C. *J. Am. Chem. Soc.* **1984**, *106*, 2439−2440.
(16) Messori, L.; Monanni, R.; Scozzafava, A. *Inorg. Chim. Acta* **1986**, L15-L17.
(17) Dickins, R. S.; Howard, J. A.; Maupin, c. L.; Moloney, J. M.; Parker, D.; Riehl, J. P.; Siligardi, G.; Gareth Williams, J. A. G. *Chem. Eur. J.* **1999**, *5*, 1095−1105.
(18) Maupin, C. L.; Parker, D.; Williams, J. A. G.; Riehl, J. P. *J. Am. Chem. Soc.* **1998**, *120*, 10563−10564.
(19) DOTMA = (1*R*,4*R*,7*R*,10*R*)-α,α′,α″,α‴-tetramethyl-1,4,7,10-tetraaza cyclododecane-1,4,7,10-tetraacetic acid; DOTA = 1,4,7,10-tetraazacyclododecane-1,4,7,10-tetraacetic acid.
(20) Brittain, H. G.; Desreux, J. F. *Inorg. Chem.* **1984**, *23*, 4459−4466.
(21) Di Bari, L.; Pintacuda, G.; Salvadori, P. *Eur. J. Inorg. Chem.* **2000**, 75−82.
(22) Aime, S.; Botta, M.; Ermondi, G. *Inorg. Chem.* **1992**, *31*, 4291−4299.
(23) The stereochemical descriptors *n* and *p* refer to the relative stereochemistry of the ring and the acetate arms in the diastereisomeric conformation of the complex.
(24) Desreux, J. F. *Inorg. Chem.* **1980**, *19*, 1319−1324.
(25) Aime, S.; Botta, M.; Fasano, M.; Marques, M. P. M.; Geraldes, C. F. G. C.; Pubanz, D.; Merbach, A. *Inorg. Chem.* **1997**, *36*, 2059−2068.
(26) Bleaney, B. *J. Magn. Reson.* **1972**, *8*, 91−100.

should be proportional to D. This is an additional critical point that will be discussed in the following.

Experimental Section

Pure Yb DOTMA as methylglucammonium salt was a gift from Bracco S.p.A. A small quantity of Yb DOTA was prepared according to Desreux.[24] Water and methanol solutions of YbDOTA and YbDOTMA were prepared at concentrations between 10 and 160 mM.

The NMR spectra were recorded on a Varian VXR spectrometer, operating at 300 MHz resonance frequency for ^{1}H. The CD and absorption spectra were measured on an upgraded JASCO 200 D spectropolarimeter, operating between 750 and 1350 nm, modified with a tandem Si/InGaAs detector with dual photomultiplier amplifier[28] and temperature control stable within ±2 °C. The bandwidth was 5 nm and further narrowing of the slit did not improve the resolution. The spectra were recorded at 10 nm/min with a time constant of 1 s, thus each acquisition required about 16 min. The pathlength was 1 cm. Only for the more diluted solutions and for the weaker lines 4 acquisitions were averaged to improve the signal-to-noise ratio.

The spectra were recorded via digital read-out equipment connected directly to the dichrograph. As the basis for resolution and curve fitting, performed with a home-built routine on KaleidaGraph (Abelbeck Software) software package, a Lorentzian function of the form

$$y = \sum_{i=1}^{m} \frac{\Delta\epsilon_i^{\max}}{\left(\frac{x - \tilde{\nu}^i}{\Delta\tilde{\nu}^i}\right)^2 + 1} \qquad (1)$$

was used, where m is the number of components of the band, $\Delta\epsilon_i^{\max}$ is the peak height, $\tilde{\nu}^i$ the energy at which the latter is observed, and $2\Delta\tilde{\nu}^i$ the peak half-height width.

To a sample in D_2O, to carry out NMR and NIR-CD measurement simultaneously, a 100-fold excess of KF (Fluka) was added to further reduce the concentration of the minor form. Both CD and NMR spectra were readily measured and did not evolve over time.

Results and Discussion

The absorption and CD spectrum of Yb DOTMA in water is shown in Figure 2. The circular dichroism is readily recorded owing to the very favorable dissymmetry g-factor (up to about 0.25 at 946 nm). In fact, the transition is magnetically allowed and it must just borrow some electric dipole moment (e.g. from a 4f−5d transition) to give rise to nonvanishing rotational strength.

One can recognize several well-resolved components, between 1045 and 920 nm, with line widths below 10 nm; they are more easily distingushed in the CD spectrum owing to sign alternation.

The signs and intensities of the sequence of bands apparent from the CD spectrum are related to the dissymmetric distribution of the atoms belonging to the organic ligand and in particular the four oxygen and four nitrogen donor atoms.

Relative Contribution of the Two Forms to the CD Spectrum. The existence of two species in solution raises the problem of determining their allied contribution to the CD spectrum, weighted for their molar fraction. In principle, the two forms might have largely different rotational strengths, to the point that a priori one might not neglect the presence of the minor component, even if its molar fraction never exceeds 10%. Moreover, one has no indication of the locations of the transitions of the *p*-form, which might or might not be degenerate with those of the *n*-form, since the two have appreciably different coordination polyhedra. One can take advantage of the reversal populations of the two forms between Yb DOTA and DOTMA. Indeed, the *p* structures of these two complexes are structurally similar, as are the *n*-forms, but what is the minor component for Yb DOTA is major for Yb DOTMA and vice versa, thus Yb DOTA can be reasonably assumed as a model for the minor form of Yb DOTMA. Naturally, being DOTA achiral, one must resort to comparing the NIR-absorption spectra, shown in Figure 3.

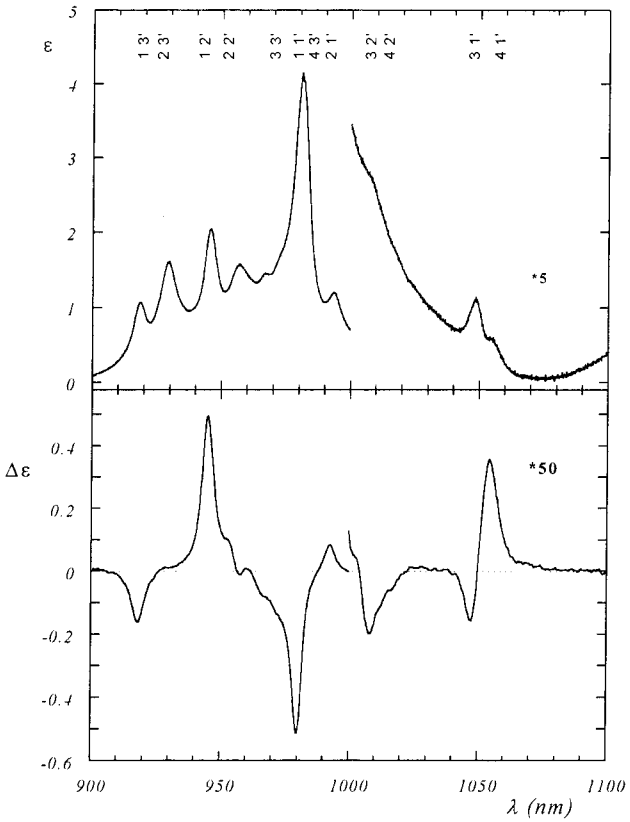

Figure 2. NIR absorption (upper curve) and CD (lower curve) spectra of YbDOTMA in H_2O (l = 1 cm, c = 0.16 M). The second part of each spectrum (1000−1100 nm region) has been expanded by a factor of 5 and 50, respectively. On the top, each line is labeled according to the assignment proposed in the text (see Figure 4): the numbers 1, 2, 3, 4 and 1′, 2′, 3′ refer to the energy levels of the $^2F_{7/2}$ and $^2F_{5/2}$ states of Yb(III) in the major form of the complex.

Although the individual intensities are somewhat different, the positions of all the bands are very similar. This leads to the conclusion that also the dichroic bands of the two forms of Yb DOTMA must be almost degenerate and that the spectrum of the *n*-type form has to be located in the same spectral region. To demonstrate that the most prominent features of the CD spectrum can be ascribed to the more abundant species only, one can displace the equilibrium position, by changing solvent composition and temperature. In particular, upon addition of a large excess of KF to the acqueous solution, the minor (*p*) form becomes much less populated (by ^{1}H-NMR it is evaluated about 2.5%), once more in reverse analogy with DOTA. The CD spectrum of this sample is superimposable to that without fluoride, which is a positive indication that it can be safely attributed essentially to the major form (see the Supporting Information). The only sizable effect of the excess of KF is a slight enlargement of the whole CD pattern, which can be related to a dependence of the crystal field parameters (see Discussion) on the ionic strenght of the solution. Moreover, also the spectrum

(27) Babushkina, T. A.; Zolin, V. F.; Koreneva, L. G. *J. Magn. Reson.* **1983**, *52*, 169−181.

(28) Castiglioni, E. *Book of Abstracts, 6th International Conference on CD*; Pisa, September 1997.

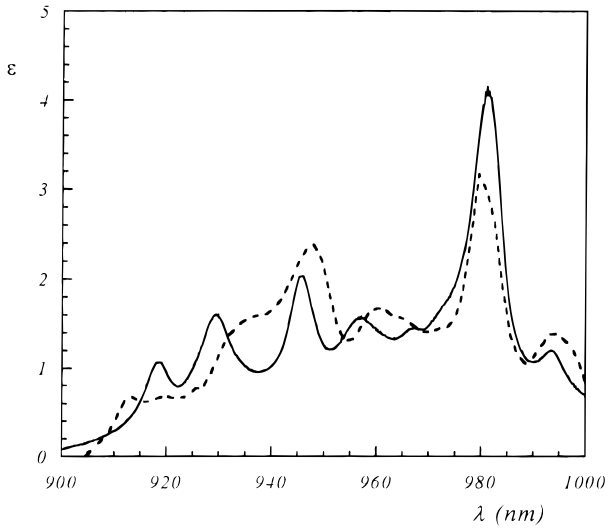

Figure 3. NIR absorption spectra (900−1000 nm region) of YbDOTA (solid line) and YbDOTMA (dashed line) in MeOH (l = 1 cm, c = 0.01 and 0.162 M, respectively).

in methanol (where the solution compostion is comparatively more favorable to the minor form) is nearly identical with that in water. From this point on, we shall assume that the minor species contributes to the main features of the CD spectrum to an extent not significantly larger than its molar fraction (i.e. that the rotational strengths of the two forms are comparable). It is noteworthy that in MeOH the counterion is partly axially bound,[21] but this does not apparently affect the electronic spectrum.

Variable-Temperature Spectra. In C_4 symmetry, the ground and excited states, $^2F_{7/2}$ and $^2F_{5/2}$, split into 4 and 3 doubly degenerate sublevels. Owing to the reduced spectral width (about 120 nm), it is likely that the splitting of the $^2F_{7/2}$ is comparable to k_BT (∼2.5 kJ mol^{-1} at 298 K) and that several levels are populated at room temperature. Indeed, one must observe that both the absorption and CD spectra are rather complex and show more than just three components (those originating from the lowest-lying level of the ground state).

To gain insight into the individual transitions of the multiplet and their rotational strengths, low-temperature spectra were recorded. At −80 °C in methanol, all the lines become narrower and appear consequently more intense, as shown in Figure 4. The position of the whole set of lines is only slightly affected and such an effect can be safely explained with structural stiffness and with a minor contribution of less defined forms as the temperature goes down.

Among the transitions observed in the CD spectrum, only four were sufficiently well-resolved to allow for a quantitative determination of rotational strengths. Rotational strenghts for these resolved transitions can be determined by integrating the observed CD in the wavenumber domain over transition profiles and then evaluating:

$$R_{ij}(T) = (2.297 \times 10^{39}) g_i \int_{i\rightarrow j} \frac{\Delta\epsilon(\tilde{\nu})}{\tilde{\nu}} \mathrm{d}\tilde{\nu} \qquad (2)$$

where $R_{ij}(T)$ denotes the rotational strenght of a transition $i \rightarrow j$, expressed in units of D^2 (D = 1 D unit = 10^{-18} esu cm); g_i is the electronic degeneracy of the level i (g_i = 2 in the present case) and the integration is over the CD profile of the $i \rightarrow j$ transition. Over a Lorentzian line shape of $\Delta\epsilon^{max}$ amplitude and $2\Delta\tilde{\nu}_i$ half-height line width, the integration of eq 2 is given by:

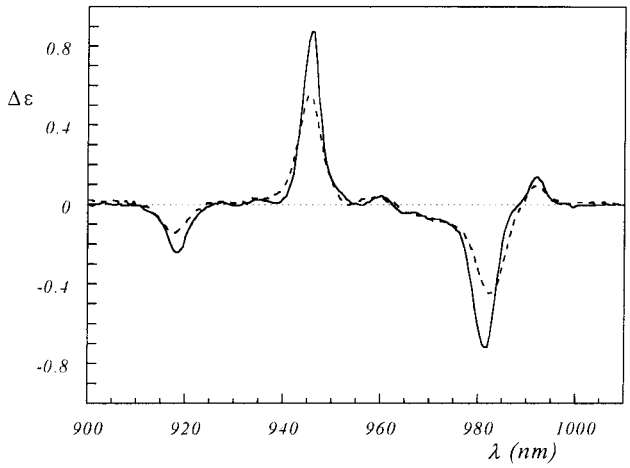

Figure 4. Variable-temperature NIR-CD spectra (900−1020 nm region) of YbDOTMA in MeOH (l = 1 cm, c = 0.096 M): 193 K (solid line) and 298 K (dashed line).

$$R_{ij}(T) = (2.297 \times 10^{39}) g_i (\pi \Delta\tilde{\nu} \Delta\epsilon^{max}) \qquad (3)$$

To this end the spectrum was deconvoluted to a sum of Lorentian line shapes, affording the data of Table 1.

Comparing the temperature-dependent rotational strengths $R(T)$ of the different transitions, one observes that the three bands at 980, 946, and 918 nm increase, while that at 993 nm becomes weaker. This is compatible with the fractional thermal populations $b(T)$ of the ground-state sublevels at room and low temperature calculated in Table 2; as a proof of our assignment of the transitions, it must be noted that the corrected rotational strenght R'

$$R' = \frac{R(T)}{b(T)} \qquad (4)$$

for the four transitions is in good approximation temperature independent (Table 1).

Tentative Assignment of the Electronic Spectrum. The splittings of the excited-state levels can be calculated from the frequencies of the three transitions assigned to the lowest-lying level as about 320 and 380 cm^{-1}. By taking into account all the transitions that can be recognized in the spectrum, one obtains the assignment depicted in the bottom of Figure 3 and in the diagram of Figure 5. This assignment is consistent with the variable-temperature data.

It is noteworthy that one component, namely the $2 \rightarrow 1'$ transition, is cleary visible in the absorption spectrum but has no detectable CD counterpart.

Interpretation of the spectrum of Yb DOTMA in terms of ligand-field effects is made difficult by the rather low number of transitions that are clearly observed in the spectrum. In C_4 symmetry, the crystal field Hamiltonian[29] can be decomposed into the sum:

$$H_{cf} = \sum_{kq} B_q^k \mathbf{C}_q^{(k)} \qquad (5)$$

where $\mathbf{C}_q^{(k)}$ are intraconfigurational spherical tensor operators of rank k (k = 2, 4, 6) and order q (q = 0, ±4 with $|q| \leq k$) and the B_q^k are the corresponding crystal fiels parameters. The whole Hamiltonian is responsible for the position of the

(29) Hüfner, S. *Optical spectra of transparent Rare Earth Compounds*; Academic Press: New York, 1978.

Table 1. Temperature Dependence of the Rotational Strenght of the Main Electronic Transitions of the Major Form of YbDOTMA in MeOH[a]

		$T = 298$ K			$T = 193$ K		
λ (nm)	transition	$\Delta\epsilon$ ($\pm$0.01)	$R(T)$ (esu^2 cm^2)	R' (esu^2 cm^2)	$\Delta\epsilon$ ($\pm$0.01)	$R(T)$ (esu^2 cm^2)	R' (esu^2 cm^2)
918	$1 \rightarrow 3'$	-0.15	-8.2 ± 0.1	-13.4 ± 0.2	-0.23	-9.1 ± 0.1	-12.9 ± 0.1
946	$1 \rightarrow 2'$	0.55	21.4 ± 0.5	34.7 ± 0.8	0.87	26.7 ± 0.5	37.7 ± 0.7
980	$1 \rightarrow 1'$	-0.45	-28.3 ± 0.3	-46.0 ± 0.5	-0.71	-31.1 ± 0.3	-44.0 ± 0.4
993	$2 \rightarrow 3'$	0.087	4.4 ± 0.1	7.2 ± 0.2	0.13	4.7 ± 0.1	6.7 ± 0.1

[a] The bands are labelled according to the assignment shown in Figure 5. $R(T)$ is the observed rotational strenght, calculated according to eq 3, R' is the corrisponding value corrected for the boltzmann factor $B(T)$ according to eq 4 (see Table 2).

Table 2. Boltzmann Populations $B(T)$ for the Crystal-Field Levels of the $^2F_{7/2}$ State of Yb in YbDOTMA

sublevel	b (298 K)	b (193 K)
1	0.616	0.718
2	0.338	0.283
3	0.029	0.005
4	0.015	0.003

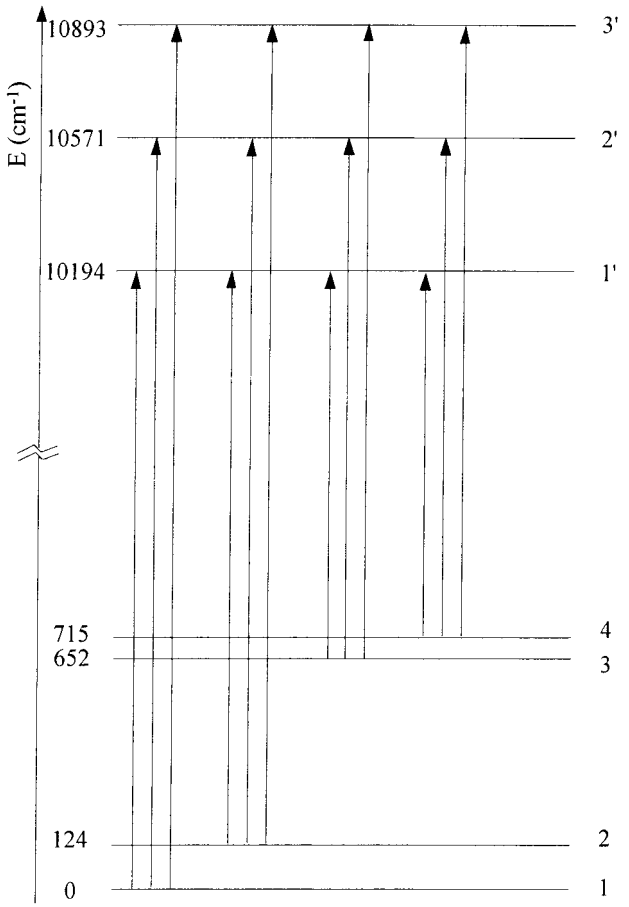

Figure 5. Electronic transition of Yb(III) in YbDOTMA (major form). The four lower levels (all doubly degenerate) belong to the $^2F_{7/2}$ state and the three upper ones to the $^2F_{5/2}$ state.

electronic transitions, it participates in determining the intensity of isotropic and dichroic bands, as well.[5] The two terms $\mathbf{C}^{(4)}_{\pm 4}$ and $\mathbf{C}^{(6)}_{\pm 4}$ in particular lead to a mixing of the M_J components of the two levels, $J = {}^7/_2$ and $J = {}^5/_2$. The values of the corresponding parameters depend on the degree of distortion of the coordination polyhedron, to the point that they are expected to vanish for C_{4v} symmetry (cubic or antiprismatic). By comparison of the absorption spectra of Yb DOTA and Yb DOTMA, we observed that the transition frequencies are nearly coincident. Considering that the two complexes differ in the layout of the atoms around the metal ion and in particular in the degree of distortion of the coordination polyhedron, it appears that the nondiagonal terms, $B^4_{\pm 4}$ and $B^6_{\pm 4}$, affect only to a minor extent the energy levels of both the ground and excited electronic states of Yb^{3+} in this complex. Another very relevant aspect emerges from this comparison, regarding the B^2_0 term. According to Bleaney,[26] it should be proportional to the magnetic susceptibility anisotropy, D. This parameter is very different for Yb DOTA and Yb DOTMA, but once more the electronic transitions span the same spectral width. These remarks lead us to the conclusion that the comparison between optical and NMR spectra can be misleading.

Conclusions and Perspectives

Ytterbium(III) ion can be used as a suitable probe to define the stereochemistry of coordinated molecules as its absorptions fall in a spectral region rather devoid of contributions from organic chromophores. In addition, NIR-CD spectra of ytterbium complexes can be recorded on suitable dichrographs with relative ease, in contrast to a somewhat common belief, since the anisotropy factors g of several components of the $^2F_{7/2} \rightarrow {}^2F_{5/2}$ term are large. In the examined complex, the sign sequence of the dichroic bands can be regarded as a direct consequence of the Λ-configuration of the coordination polyhedron. The spectrum of YbDOTMA is similar to another example of NIR-CD of a formal DOTA-derivative that recently appeared in the literature, even if the latter spectrum shows extensive band overlap.[17]

The analysis of the spectrum presented here will hopefully serve as a building block to a more nonempirical approach to the problem of the NIR transitions of this ion. A very relevant application of this spectroscopy will probably be found in the study of effects induced following interactions with chiral biological molecules.[30−34] As an example, it is well-recognized that several contrast agents for MRI do interact with plasma proteins,[35−38] which in turn are often highly stereodiscriminating and can induce preferential enantiomeric conformations.[39,40] Surprisingly, no systematic study on the role of the absolute

(30) Aime, S.; Botta, M.; Geninatti Crich, S.; Terreno, E.; Anelli, P. L.; Uggeri, F. *Chem. Eur. J.* **1999**, *5*, 1261−1266.
(31) Zitha-Bovens, E.; van Bekkum, H.; Peters, J. A.; Geraldes, C. F. G. C. *Eur. J. Inorg. Chem.* **1999**, 287−293.
(32) Shery, A. D.; Zarzycki, R.; Geraldes, C. F. G. C. *Magn. Reson. Chem.* **1994**, *32*, 361−365.
(33) Aime, S.; Bettinelli, M.; Ferrari, M.; Razzano, E.; Terreno, E. *Biochim. Biophys. Acta* **1998**, *1385*, 7−16.
(34) Govenlock, L. J.; Mathieu, C. E.; Maupin, C.; Parker, D.; Riehl, J. P.; Siligardi, G.; Williams, J. A. G. *Chem. Commun.* **1999**, 1699−1700.
(35) Aime, S.; Botta, M.; Fasano, M.; Terreno, E. *Chem. Soc. Rev.* **1998**, *27*, 19−29.
(36) Aime, S.; Botta, M.; Fasano, M.; Geninatti Crich, S.; Terreno, E. *JBIC* **1996**, *1*, 312−319.
(37) Kirchin, M. A.; Pirovano, G. P.; Spinazzi, A. *Invest. Radiol.* **1998**, *33*, 798−809.
(38) Cavagna, F. M.; Maggioni, F.; Castelli, P. M.; Daprà, M.; Imperatori, L. G.; Lorusso, V.; Jenkins, B. G. *Invest. Radiol.* **1997**, *32*, 780−796.
(39) Kragh-Hansen, U. *Pharmacol. Rev.* **1981**, *33*, 17−53.
(40) Salvadori, P.; Bertucci, C.; Ascoli, G.; Uccello-Barretta, G.; Rossi, E. *Chirality* **1997**, *9*, 495−505.

stereochemistry of contrast agents could be found in the literature, although a slowly increasing number of chiral complexes has been developed.[17,18,41,42] One possible reason is the lack of analytical tools for sensing the configuration around the metal ion and hopefully CD and CPL of lanthanide ions and in particular of ytterbium will provide the missing information. Moreover, coupling near-infrared chiroptical methods and NMR of paramagnetic Yb^{3+} labile complexes will eventually provide a powerful tool for investigating interactions between biomolecules and lanthanides, which in turn can give inportant information on Ca^{2+} binding.

Acknowledgment. Dr. Fulvio Uggeri, Bracco S.p.A. is thanked for a sample of Yb DOTMA. We are also indebted to Dr. Ettore Castiglioni, JASCO Italy, for constant and prompt assistence with the spectropolarimeter.

Supporting Information Available: NIR CD spectrum of YbDOTMA in D_2O solution and 1.6 M KF and difference between the two spectra with and without KF in solution (Figure S1) (PDF). This material is available free of charge via the Internet at http://pubs.acs.org.

JA994290Z

(41) Howard, J. A. K.; Kenwright, A. M.; Moloney, J.; Parker, D.; Peacock, R.; Siligardi, G. *J. Chem. Soc., Chem. Commun.* **1998**, 1381−1382.

(42) Aime, S.; Barge, A.; Bruce, J. I.; Botta, M.; Howard, J. A. K.; Moloney, J. M.; Parker, D.; de Sousa, A. S.; Woods, M. *J. Am. Chem. Soc.* **1999**, *121*, 5762−5771.